LBL-25817
UC-210

Lawrence Berkeley Laboratory
UNIVERSITY OF CALIFORNIA

APPLIED SCIENCE DIVISION

LAWRENCE
BERKELEY LABORATORY
DEC 2 1988
LIBRARY AND
DOCUMENTS SECTION

Technology Base Research on the Slurry-Zinc/Air Battery System: Final Report

H.B. Sierra Alcázar, P.D. Nguyen, and A.A. Pinoli

August 1988

APPLIED SCIENCE
DIVISION

Prepared for the U.S. Department of Energy under Contract Number DE-AC03-76SF00098.

LBL-25817

DISCLAIMER

This document was prepared as an account of work sponsored by the United States Government. While this document is believed to contain correct information, neither the United States Government nor any agency thereof, nor the Regents of the University of California, nor any of their employees, makes any warranty, express or implied, or assumes any legal responsibility for the accuracy, completeness, or usefulness of any information, apparatus, product, or process disclosed, or represents that its use would not infringe privately owned rights. Reference herein to any specific commercial product, process, or service by its trade name, trademark, manufacturer, or otherwise, does not necessarily constitute or imply its endorsement, recommendation, or favoring by the United States Government or any agency thereof, or the Regents of the University of California. The views and opinions of authors expressed herein do not necessarily state or reflect those of the United States Government or any agency thereof or the Regents of the University of California.

LBL-25817

TECHNOLOGY BASE RESEARCH ON THE SLURRY-ZINC/AIR BATTERY SYSTEM

Final Report

August 1988

by

H.B. Sierra Alcázar
P.D. Nguyen
A.A. Pinoli

Pinnacle Research Institute
10432 N. Tantau Avenue
Cupertino, California 95014

for

Technology Base Research Project
Applied Science Division
Lawrence Berkeley Laboratory
1 Cyclotron Road
Berkeley, California 94720

This work was supported by the Assistant Secretary for Conservation and Renewable Energy, Office of Energy Storage and Distribution, Energy Storage Division of the U.S. Department of Energy under Contract No. DE-AC03-76SF00098, Subcontract No. 4543210 with the Lawrence Berkeley Laboratory.

EXECUTIVE SUMMARY

Characteristics of the secondary slurry-Zn/air battery at the single-cell level have been studied in this project. The objectives of the second year of funding were to improve the capacity, specific energy, and specific power of the discharge process as well as to develop an efficient slurry recharge method. The overall goal of this program is to demonstrate, with models based on single-cell experimental data, the capability of the slurry-Zn/air battery to power electric vehicles (EV's) with recharge energy supplied through various modes. The recharge modes considered include (a) hydraulic recharge, by replacing the fluidized anode, (b) on-board electrical recharge (slow or fast) in a separate cell, and (c) a combination of hydraulic recharge with electric recharge of spent electrolyte at central stations.

The second year program advanced the state of the art in terms of increased discharge capacity and cell performance. A passivation problem with the air cathode was identified, and the inherent discharge capacity (independent of air cathode passivation) was determined in the process of selection and optimization of discharge-capacity-extension additives. The discharge performance was improved with the design of bi-cell II. Critical data to model a secondary slurry Zn-Air battery was also determined in a cell with a manually scraped cathode for dendritic Zn production. The effects on recharge of current density, temperature, cathode substrate, hydrodynamics, depth of charge (DoC), and capacity extension additives were ascertained. These results will be used to design a practical recharge cell.

Calculations for a 50 kW, 755 kg secondary slurry-Zn/air battery system for the IDSEP van were carried out. The modeling assumed 100 % DoD, based on the inherent capacity of the 12 M KOH electrolyte utilizing 25 g/l LiOH as an additive, and a constant discharge voltage vs. DoD curve. The projected energy density at 5.5 kW (cruising power) is 180 Wh/kg. For slow recharge the round trip calculations show >99 % coulombic efficiency, 54 % voltage efficiency and 47 % energy efficiency. The estimated cost of energy is $0.14 per kg of Zn recharged with off-peak electrical energy at $0.07 per kWh. If H_2, costing $1.67/100 SCF, is used to depolarize the anodes of a central recharge reactor, the cell voltage can be reduced from 2.3 V (on board reactor) down to 0.7 V with H_2 oxidation at 75 mA/cm^2. Therefore the consumption of electrical energy is reduced and the total cost of recharge energy is then only $0.06 per kg of Zn, i.e. $0.056/kWh.

The discharge experiments suggest that substantial improvements in discharge capacity can be obtained by preventing passivation of the air cathode. A new design of the discharge cell should be attempted in phase III, incorporating a separated catholyte compartment. The new cell design should attempt to increase turbulence, improve flow distribution and minimize pressure losses. A consistent improvement in capacity has been achieved with additives for the past two years; it is recommended that this effort be continued in phase III.

A practical recharge cell with automatic scraping of dendritic Zn from a planar Mg cathode needs to be constructed in phase III. The recharge experiments have provided the basis for its design: It has been learnt that the current density levels should match the zincate concentration (DoC) to minimize recharge energy, and that quiescent conditions and a Mg cathode substrate favor dendritic Zn deposition. The region of temperature, current density and zincate concentration at which the energy and power requirements for recharge are minimum needs further exploration to delineate the limits between acceptable (dendritic) and non-acceptable deposit morphology. It is recommended that further refinements of the recharge cell (i.e. hydrogen depolarization) and coupling to the discharge cell for cycling be accomplished at the single cell level before proceeding to scale up developments.

Contents

EXECUTIVE SUMMARY ---------- i

1. INTRODUCTION ---------- 1
   Description of System ---------- 1

2. EXPERIMENTAL ---------- 3
   2.1 Discharge Bi-Cell II ---------- 4

3. ADDITIVES TO INCREASE DISCHARGE CAPACITY ---------- 5
   3.1 Capacity Extension Obtained with the Air Bi-Cell ---------- 5
   3.2 Inherent Discharge Capacity Obtained with the Transition Time Method ---------- 9

4. DISCHARGE PERFORMANCE ---------- 13
   4.1 Air Cathode Passivation ---------- 13

5. RECHARGE PERFORMANCE ---------- 17
   5.1 Recharge Studies ---------- 17
   5.2 Manually Scraped Recharge Cell ---------- 19
   5.3 Coulombic Efficiency ---------- 19
   5.4 Cell Voltage ---------- 21
   5.5 Current Density and Deposit Morphology ---------- 21
   5.6 Half Cell Energy Density ---------- 21
   5.7 Temperature Effects ---------- 23
   5.8 Hydrodynamic Conditions Effects ---------- 23
   5.9 Current Waveform Effects ---------- 25
   5.10 Cathode Substrate Effects ---------- 25
   5.11 Effect of Discharge Additives ---------- 27

6. MODELING OF Zn-AIR BATTERY SYSTEMS ---------- 29
   6.1 11-KW Hydraulically Recharged Slurry-Zn/Air Battery System ---------- 29
   6.2 60-KW Hydraulically Recharged Slurry-Zn/Air Battery System ---------- 29
   6.3 50-KW Slurry-Zn/Air Battery System with On-Board Recharge ---------- 29

ACKNOWLEDGEMENT ---------- 35

REFERENCES ---------- 35

1. INTRODUCTION

The slurry-Zn/air battery system has received renewed R & D interest (1-8) because it does not have the shape-change problems of batteries with Zn-plate electrodes and can sustain higher current densities and specific peak power than other metal-air battery systems. Additional advantages of the slurry-Zn/air battery include safety, low environmental impact, potential low cost, and separation of energy density from power density functions for design purposes. In this work we present results obtained at the individual cell level (3,4,5,7) as a basis to estimate the performance of a secondary slurry-Zn/air battery system (7). The expected specific energy of such systems has been increased as a result of the use of capacity-extension additives, which has been one of the major thrusts of this work .

1.1 Description of System

The slurry Zn-Air battery system is a good candidate to power electrical vehicles, either with hydraulic or electric recharge or with both. Hydraulic recharge can be accomplished at strategically located stations by replacing spent electrolyte with a fresh slurry of KOH solution and Zn particles. The spent electrolyte consisting of KOH solution with dissolved zincate (term employed to designate $Zn(OH)_4^-$ species, micelles with ZnO, and dissolved polymeric species containing ZnO) can be electrically recharged at a separate recharge reactor which can be carried on board. Deposition of dendritic Zn on a suitable substrate, such as Mg or glassy carbon plate, can be performed in a central-station recharge reactor, with the added advantage of cheap sources of energy (i.e., night-rate electric energy and hydrogen to depolarize the anode). The Zn powder can be integrated into the electrolyte (with very low zincate concentration) by mechanical scraping of the dendrites from the cathode substrate plates of either an on-board recharge reactor or a central- station recharge reactor.

The secondary slurry-Zn/air battery system is envisioned as comprising separate discharge and recharge reactors, as schematically shown in Figure 1. The slurry of dendritic Zn particles is recirculated through the discharge reactor with the help of a centrifuge pump. The recharge reactor will most likely benefit from operation under quiescent conditions, and could be located inside

of the slurry reservoir tank (Tank No. 1). An additional Tank No. 2, is envisaged to carry either fresh slurry (with very little zincate) or KOH electrolyte which can be fed to the discharge reactor in order to cope with peak-power requirements. The fresh slurry can be circulated once through the discharge reactor and mixed into Tank No. 1, thereby cleaning the air cathode from precipitated ZnO which dissolves in the fresh electrolyte. Alternatively, Tank No. 2, provides KOH solution which functions as a catholyte feed to a discharge cell with separated catholyte compartments. The cell with separated catholyte should in principle be capable of sustained maximum power at all stages of discharge.

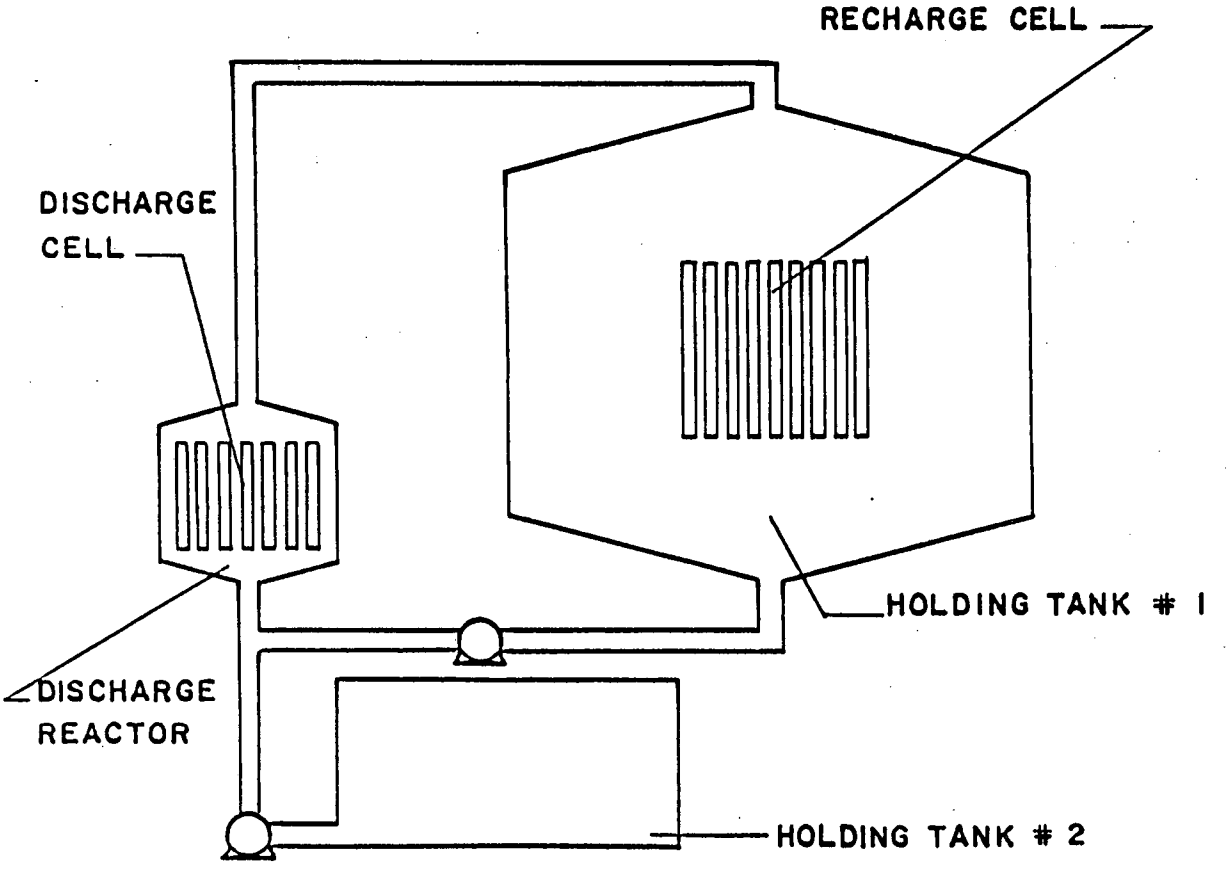

Figure 1. Diagram of a secondary slurry-Zn/air battery system.

2. EXPERIMENTAL

A detailed description of the experimental procedures has already been published (1,5), thus only the new developments will be addressed here. A diagram for the discharge system used in the capacity and performance studies of bi-cell II is shown in Figure 2. The air is passed through a hot 12 M KOH solution prior to entering the air cathode in order to remove CO_2 and to preheat and humidify it. The flow rate was monitored with a mass flow transducer, and the air flow rates were adjusted to 4.5 times the oxygen stoichiometric requirements. The air back pressure was controlled by submersing the air output hose from the bi-cell to the desired depth (a few inches) in a column filled with water. The electrolyte back-pressure could be varied by controlling the height of electrolyte in a reservoir tank above the bi-cell, and the electrolyte reservoir tank could also be pressurized externally through the venting port, but this option was not used in the experiments. The Zn powder was maintained in suspension at all times by recirculating the electrolyte and Zn powder slurry. The slurry flow was distributed with the help of a single or multiport nozzle at the bottom of the bi-cell holding tank.

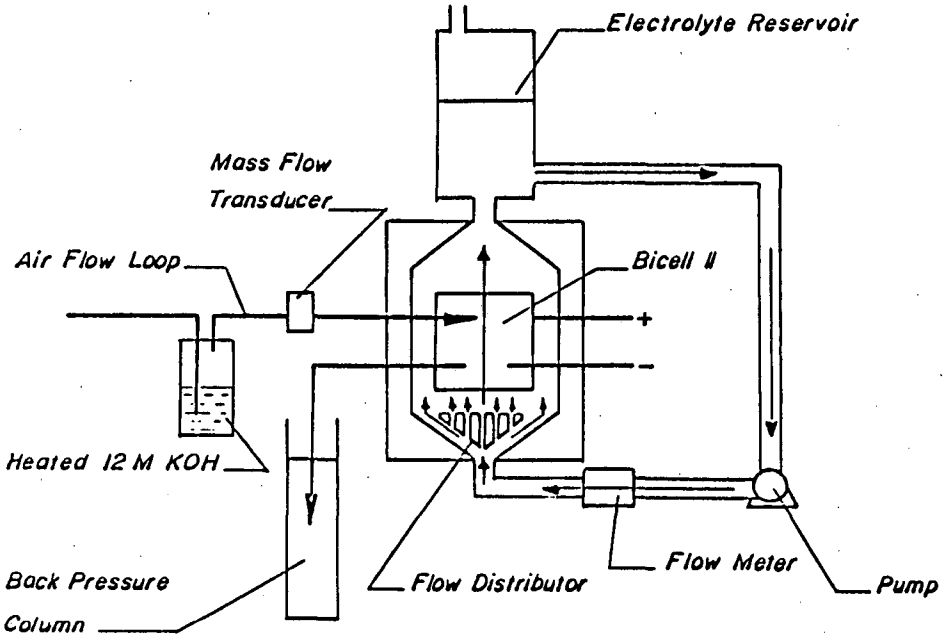

Figure 2. Discharge system for bi-cell II

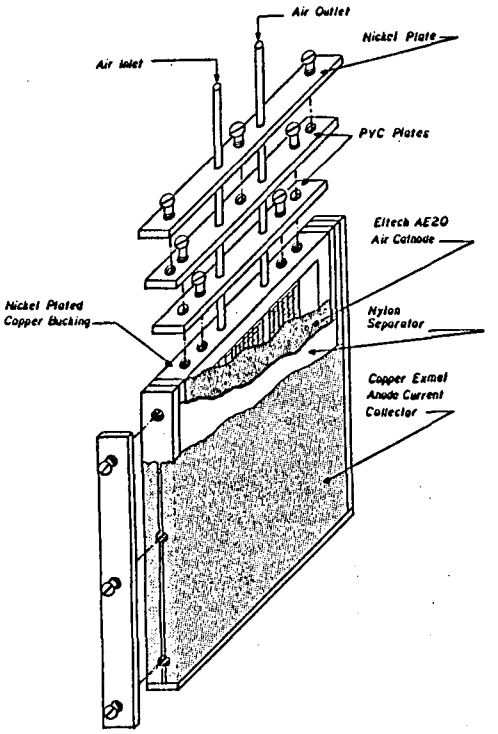

Figure 3. Diagram of bi-cell II

The overall flow rate could be measured with a propeller-type flow meter. The holding tank for the bi-cell allowed a 0.7-cm gap between its walls and the bi-cell.The slurry flowed upwards (with some eddies) in this channel with no agglomeration problems. The air ports and feedthroughs for electrical connections were on the sides of the holding tank, and a bigger port allowed the introduction of the bi-cell through one side of the tank.

2.1 Discharge Bi-Cell II

A diagram of bi-cell II is presented in Figure 3. This design is slimmer, lighter, and has better hydrodynamic flow than bi-cell I, but it has the same planar configuration. The electrodes are arranged on both sides of a copper frame in the following order from the inside out: gas diffusion cathode (AE20 or AE100 models from Electromedia Corp.), nylon cloth separator, and copper exmet serving as current collector for the Zn slurry anode. The air (or pure oxygen) flowed in and out of the cavity formed by the copper frame and the two interconnected air cathodes. The design of bi-cell II allowed the removal of the frame and ribs that were present on the outside of the Copper exmet of bi-cell I, thereby improving the flow characteristics of the slurry. The capacity determined with bi-cell II showed a 32% improvement over that determined with bi-cell I, as can be seen in Figure 4 and Table 1 for the case of the additive containing silicate and sorbitol.

3. ADDITIVES TO INCREASE DISCHARGE CAPACITY

The use of electrolyte additives to improve discharge capacity was investigated. These additives were selected to obtain a high oversaturation of zincate ion in KOH electrolyte. The mechanisms by which the additives extend the discharge capacity was discussed in a recent publication (2).

3.1 Capacity Extension Obtained with the Air Bi-Cell

Improvements in the discharge capacity which were obtained during Phases I and II are shown in the bargraph of Figure 4 and in Table 1. It is clear that improvements have been achieved because of the use of additives and improvements in cell design. The specific capacity of pure 12 M KOH determined with a 200-cm^2 bi-cell (2) was 106 Ah/l (87 g Zn^{++}/l). The capacity can be increased by adding a type A additive (25 g/l silicate) to aid in the formation of micelles around minute particles of ZnO. A further increase in specific discharge capacity to 203 Ah/l (248 g Zn^{++}/l) can be obtained by combining with a Type B additive (25 g/l silicate + 15 g/l sorbitol) that helps stabilize polymeric chains involving ZnO molecules (2,3). The highest discharge specific capacity was 228.8 Ah/l (279 g Zn/l), which was obtained with 25 g/l LiOH in 12 M KOH (4,10). However, it is not clear yet how LiOH extends the specific discharge capacity.

The capacity obtained by discharging with an air cathode in a static catholyte is not the maximum that could be obtained because the porous air cathode passivated before the circulating anode (Zn particles) did (4,7). The most likely mechanism of passivation is ZnO precipitation inside the air cathode pores due to a decreased concentration of water in the electrolyte. The water is depleted at the cathode because it reacts with O_2 to form OH^-. Figure 5 shows change in the anode and cathode potentials with depth of discharge. It is clear that the cathode limits the capacity of the electrolyte, before the anode potential gives signs of deterioration. Unity (1.0 fractional DOD) depth of discharge in Figure 5 corresponds to the inherent discharge capacity, as further explained in the next section.

The increase in discharge capacity is mainly responsible for the excellent energy density characteristics projected for battery models (see section 6). The factors contributing to the increased capacity are the effect of capacity extension additives

TABLE 1. EFFECT OF ADDITIVES ON DISCHARGE CAPACITY

ADDITIVE	MECHANISM TYPE	CATHODE LIMITED CAPACITY* g Zn^{++}/L (AH/L)	INHERENT CAPACITY** g Zn^{++}/L (AH/L)
25 g/L LiOH	D	279.0 (228.8)	368.5 (302.2)
15 g/L LiOH	D		310.2 (254.4)
10 g/L LiOH	D		315.6 (258.8)
5 g/L LiOH	D		314.6 (258.0)
25 g/L SILICATE, 15 g/L SORBITOL	A,B	248.0 (203.4)	293.0 (240.3)
15 g/L SORBITOL	B	172.5 (141.49)	
25 g/L SILICATE	A	187.5 (153.8)	
SATURATED STANNATE	A	170.4 (139.77)	
25 g/L ALUMINATE	A	151.8 (124.54)	
SATURATED TITANATE	A	124.6 (102.22)	
12M KOH, NO ADDITIVE	-	106.3 (87.2)	
3M KOH, 15 g/L SILICATE	C	78.6 (64.5)	
3M KOH, 25 g/L SILICATE	C	84.3 (69.2)	
3M KOH, 100 mA/cm^2, 15 g/L SILICATE	C	74.1 (60.8)	
3M KOH, 25°C, 15 g/L SILICATE	C	90.2 (74.0)	

* ALL EXPERIMENTS WERE PERFORMED AT 200 mA/cm^2, 12 M KOH AND 55°C, UNLESS OTHERWISE INDICATED.

** INHERENT CAPACITY WAS CALCULATED BASED ON ROTATING DISC EXPERIMENTS AT ROOM TEMPERATURE AND 1000 RPM.

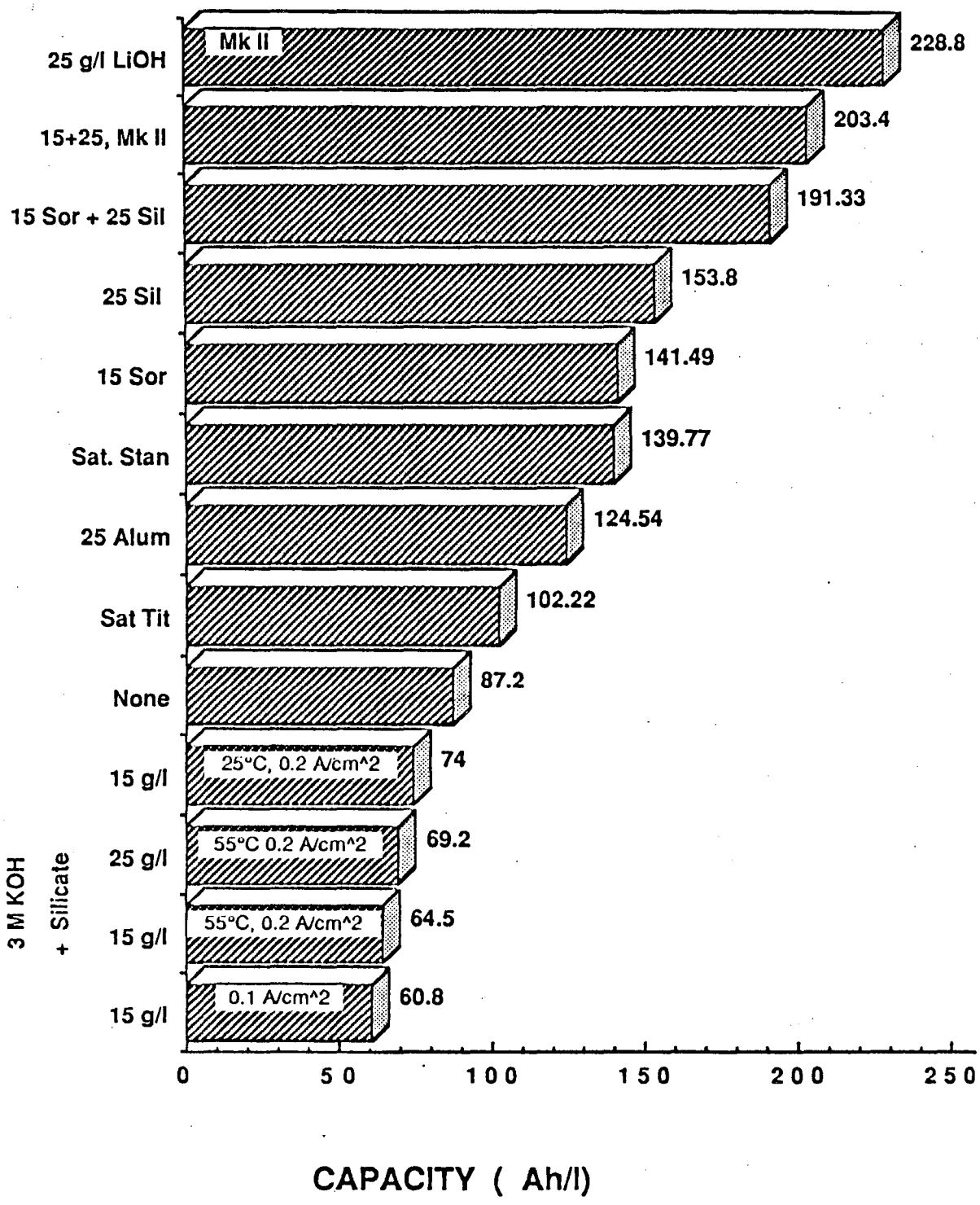

Figure 4. Discharge Capacity obtained with additives. Discharge experiments performed at 55°C, 200 mA/cm², in 12 M KOH unless otherwise specified.

and the improved hydrodynamic conditions of the slurry anode in bi-cell II with respect to those of bi-cell I.

For a given capacity extension additive, passivation of the Zn particles depends on the transport characteristics of the system closely associated with hydrodynamic conditions. The discharge capacity is then a function of the instantaneous current density, time, and space-averaged potential of the particles; concentration of metallic Zn, KOH and zincate in the slurry electrolyte; thickness of diffusion layer, residence time in the discharge reactor, friction and mechanical effects of impellers that might split particles or knock out passive layers; characteristics of anode current collector that might influence the time averaged size and number of Zn particle chains; size distribution, and morphology of Zn particles that might affect the real current density (by affecting the average collision rate and surface of particles).

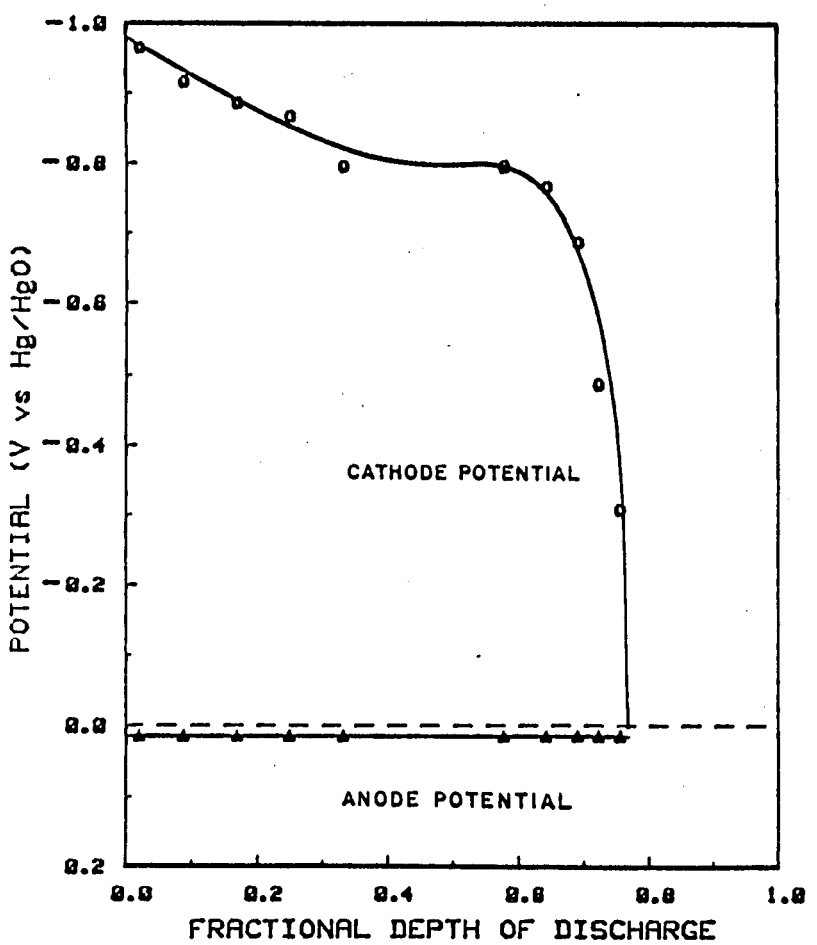

Fig. 5. Cathode and anode potential profile with respect to fractional depth of discharge. Profiles were obtained at 200 mA/cm^2, 12 M KOH, 55°C with 25 g/l LiOH as the additive.

3.2 Inherent Discharge Capacity Obtained with the Transition Time Method (TTM)

A useful method to evaluate the inherent discharge capacity (IDC) extension provided by additives, independently of the behavior of the air electrode, was developed. The method is based on the determination of the passivation time, t_p, of a Zn rotating disk electrode in the test electrolyte. A critical current density, i_c, was determined as a function of zincate concentration and additive concentration from the t_p measurements (4,7) that followed the Sand equation $i_c = k/\sqrt{t_p}$. The concentration of zincate at which the critical current density becomes zero defines the IDC extension of the additive. The IDC was extrapolated from the concentration vs.critical current density curve for various additive concentrations; a summary of inherent discharge capacities and discharge capacities from the bi-cell measurements (Mark I and II) is given in Table 1.

The IDC was extrapolated from the concentration vs.critical current density curve for various additive concentrations. The experimental results for a combination of Type A and B additives are shown in Fig. 6 It is clear that the Sand equation is followed and can be used to determine the critical current density, i_c, as a function of zincate concentration.

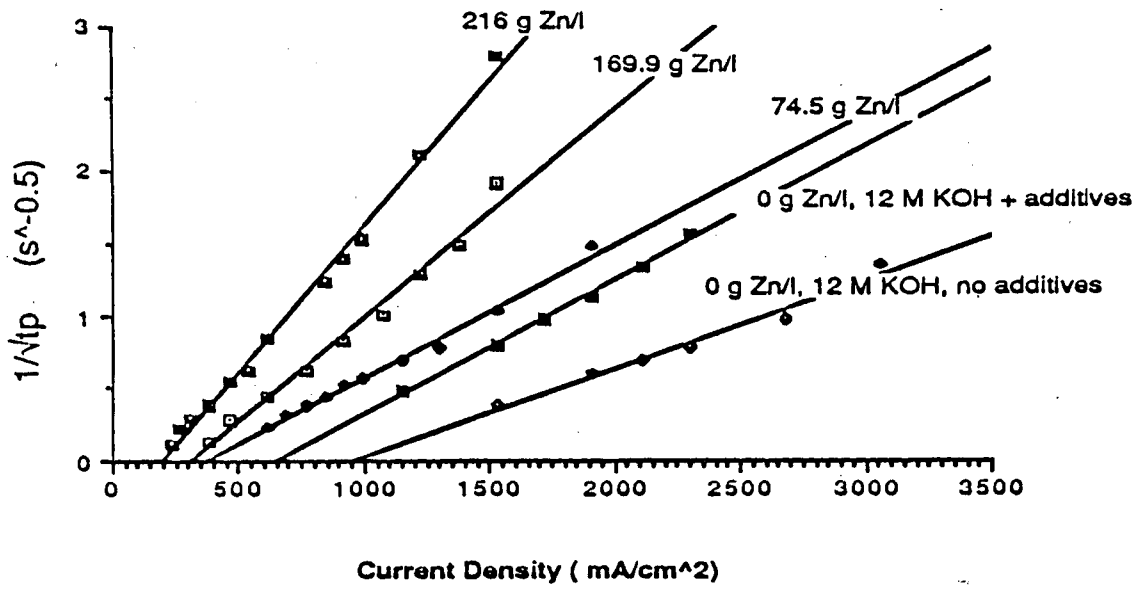

Fig. 6. Variation of time to passivation with current density at various zincate concentration in 12 M KOH and 25 g/l silicate, 15 g/l sorbitol at room temperature at 1000 rpm.

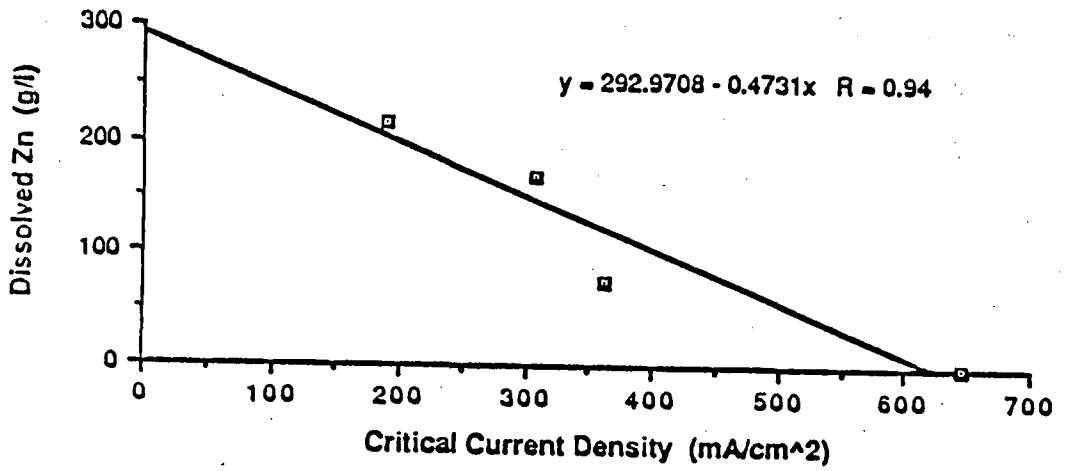

Fig. 7. The effect of zincate concentration on critical current density at 12 M KOH plus 25 g/l silicate and 15 g/l sorbitol.

The concentration of zincate at which the critical current density becomes zero defines the inherent capacity extension of the additive combination for the particular temperature and hydrodynamic conditions, as illustrated in Figure 7. The maximum IDC of 25 g/l silicate + 15 g/l sorbitol additives was 293 g Zn/l, extrapolated from the concentration vs.critical current density curve.

The TTM is useful for screening and optimizing additives. It was used to determine the concentration of LiOH additive to 12 M KOH that rendered the highest IDC; the best results were obtained with a LiOH concentration of 25 g/l. The corresponding $1/\sqrt{t_p}$ vs. current density curves are shown in Figure 8. From this figure the critical current densities were extrapolated and plotted in Figure 9 against concentration of dissolved Zn in the electrolyte. The IDC at room temperature and 1000 RPM, extrapolated from Figure 9 at zero critical current density, was 302 Ah/l (368.5 g Zn/l), which is the highest value obtained with any of the additives and additive combinations tested.

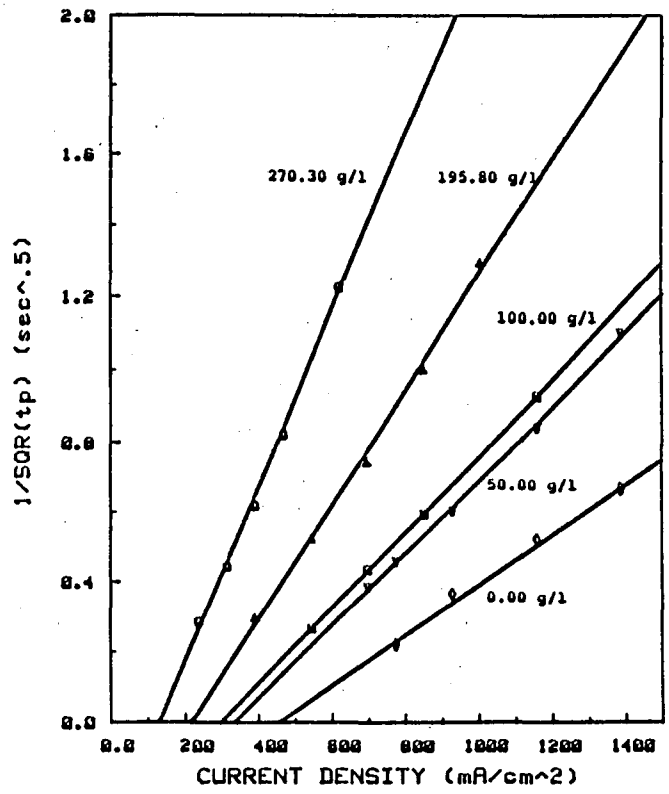

Fig. 8. Inverse square root of passivation time vs current density. Experiments were performed in a rotating disc apparatus with an electrode area of .1307 cm^2, and rotating speed of 1000 rpm. 25 g/l of LiOH , and various concentration of Zn^{++} in 12 M KOH were used as the electrolyte.

This 302 Ah/l is the value used as 100 % DoD in the modeling calculations and represents an improvement of 32% over the air cathode limited discharge capacity of 228.8 AH/l (279 g Zn/l) obtained with bi-cell II (with static, non-separated catholyte). The discharge capacity improvement can be expected to became a reality in functional cells by preventing the build up of zincate ions in the catholyte inside the air cathode. This is one of the goals of the Phase III research effort. This goal could be accomplished either with a flowing catholyte or with periodic flushings with fresh KOH solution, which was stored in a separate tank. As a final alternative, catholyte contamination with zincate could be avoided by separating the anolyte from the catholyte with a permselective membrane.

Confidence in the TTM as an additive selection tool was reinforced by noting (see Table 1) the same ranking of additives obtained with the capacity determination experiments performed with bi-cell II.

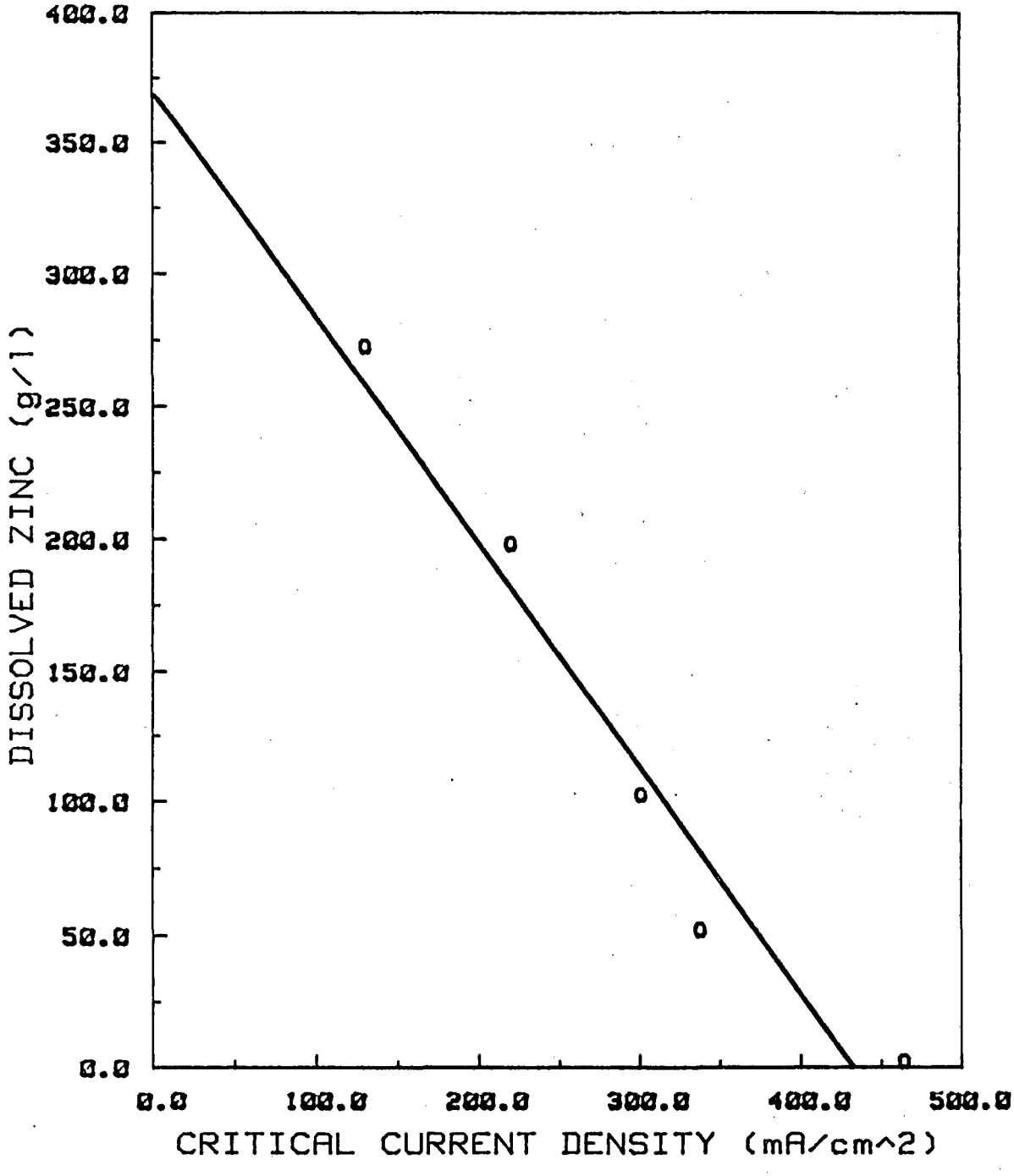

Fig. 9. Dissolved Zn vs Critical Current Density (Inherent capacity for 25 g/l LiOH)

4. Discharge Performance

4.1 Air Cathode Passivation

The cell voltage obtained by discharging with the air cathode in its present condition is not optimized because the air cathode passivates before the circulating anode (Zn slurry) does, as shown in Figure 5. Therefore the peak specific power (with respect to exposed area of the air cathode) obtained during discharge is a function not only of current density but also of DoD. Figure 10 shows cell voltages versus current density curves obtained with bi-cell II containing a silicate + sorbitol additive combination, near zero DoD. Very similar performance with oxygen and air depolarization was obtained when using Zn powder slurry; the use of Zn coated polymeric beads (Sorapec) rendered lower cell voltages, as reported earlier (5) . The corresponding specific power (with respect to air cathode projected area) versus current density curve is shown in Figure 11. It can be seen that 483 mW/cm^2 peak power was obtained with pure oxygen and 444 mW/cm^2 peak power was obtained with air depolarization, using Zn powder slurry with 15 g/l sorbitol and 25 g/l silicate additives. The peak power obtained with Sorapec beads was about 360 mW/cm^2 in similar conditions.

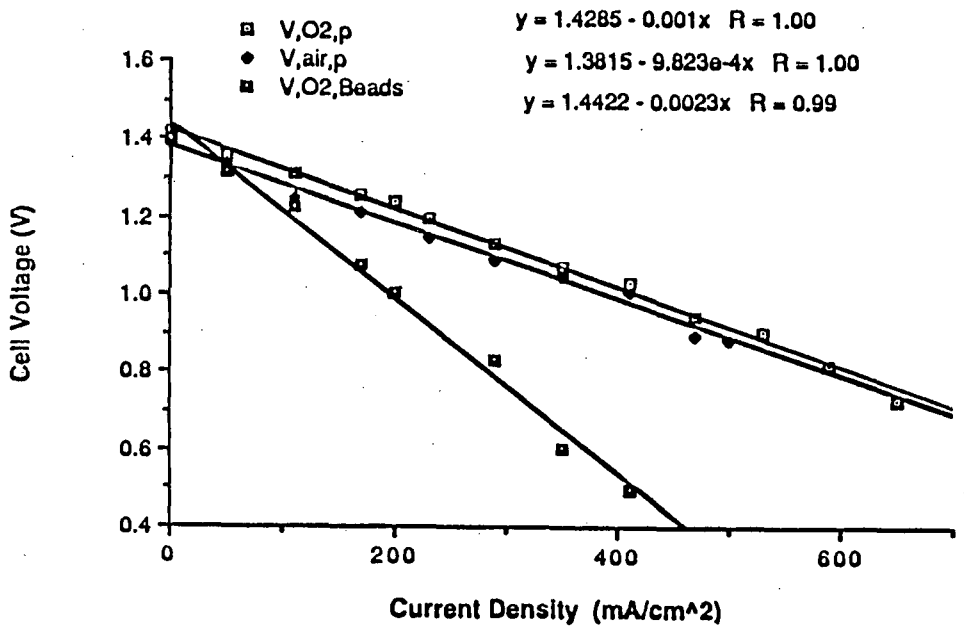

Figure 10. Cell Voltage versus current density curves of bi-cell II Discharge of Sorapec beads and Zn powder slurries in 12 M KOH with 25 g/l SiO_2 and 15 g/l Sorbitol. Pure O_2 or air flowing at 4.5X the Stoichiometric ratio was used as cathode depolarizer.

Figure 12 shows the cell potential versus current density curves taken at various DoD, with 25 g/l LiOH additive in the 12 M KOH starting electrolyte. The cell potential decay with DoD was mainly due to the decrease in the cathode potential, as shown in Figure 5. The corresponding specific power vs. current density curves as a function of DoD are shown in Figure 13. The discharge performance deteriorated with depth of discharge primarily due to air cathode passivation; for example a peak power of 810 mW/cm^2 was obtained at 0% DoD. A steep decay in peak power started at about 20% DoD down to 243 mW/cm^2 at 60% DoD (25 g/l LiOH additive, O_2 depolarization). The maximum peak power is probably somewhat higher than 810 mW/cm^2 because the curve does not appear to have reached a maximum at 800 mA/cm^2 (measurements stopped at 40 A, which is the current limit of the power supply used to discharge at constant current density)

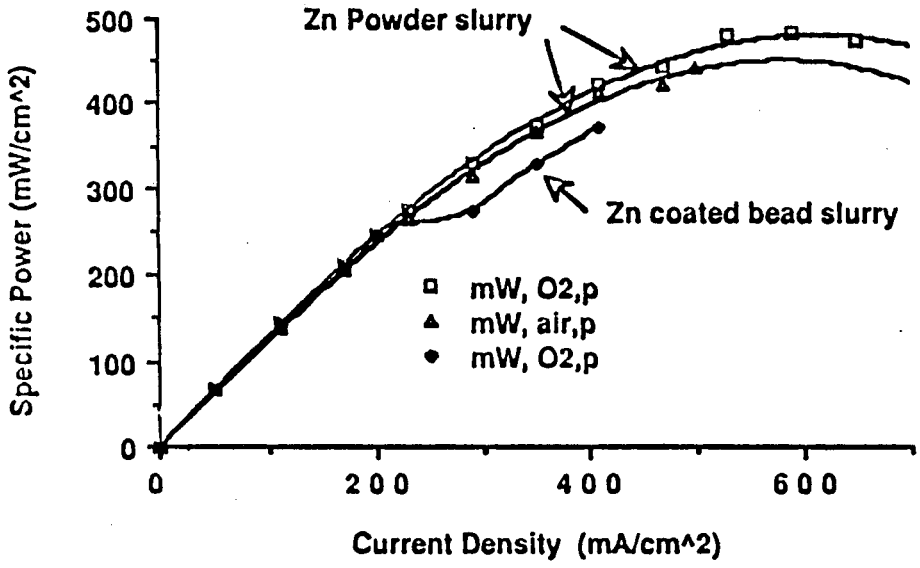

Figure 11. Specific Power versus current density curves of bi-cell II corresponding to discharge of slurries Zn powder or Sorapec beads in 12 M KOH with 25 g/l SiO_2 and 15 g/l sorbitol at 55°C. Pure O_2 or air flowing at 4.5X the stoichiometric ratio was used as cathode depolarizer.

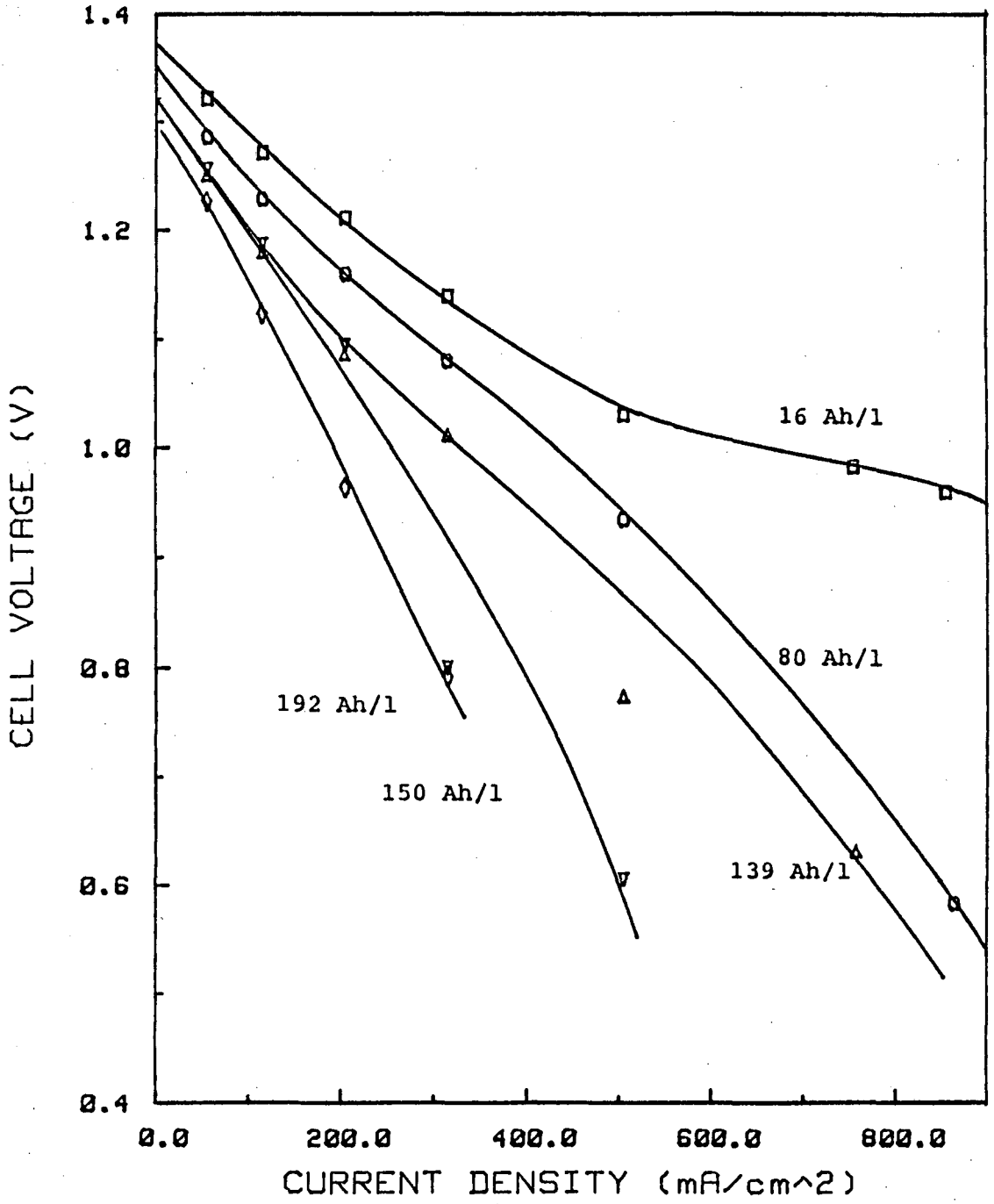

Fig. 12. Cell potential vs Current density with respect to DoD. Polarization was performed at 55°C, 12 M KOH, 350 g/l fresh Zn, and oxygen as cathode depolarizer.

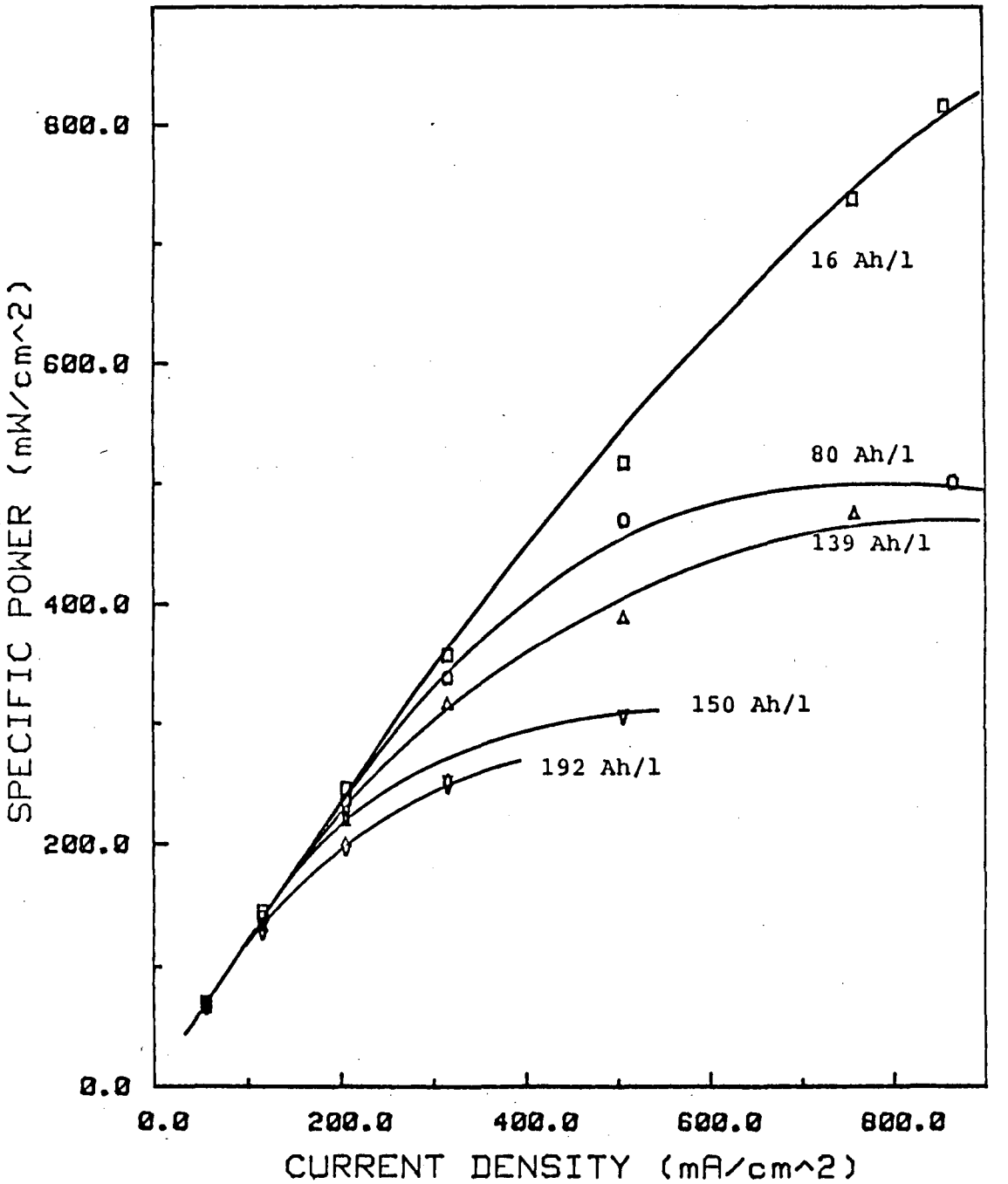

Fig. 13. Specific power vs Current density with respect to DoD. Polarization was performed at 55°C, 12 M KOH, 350 g/l fresh Zn and oxygen as cathode depolarizer.

5. RECHARGE

Operating the slurry-Zn/air system as a secondary battery may require a separate recharge cell. Deposition of Zn on scraped planar electrodes was found to be the most practical method to produce dendritic Zn powder (scraping was done manually at this stage). A Zn cathode substrate was found unsuitable because of Zn adhesion problems, but glassy carbon (GC) and Mg substrates allowed easy scraping of dendritic Zn deposits. Mg substrates required lower energy (lower half-cell energy density) than GC, therefore the studies focused on Mg substrates.

Potentiostatic, galvanostatic and galvanodynamic experiments were performed with a planar, manually scraped Mg electrode and on a rotating cylindrical Mg electrode. Deposition experiments with the planar electrode were performed at constant current and at linearly increasing ramped current (using various ramping rates). With the rotating cylinder electrode, deposition was performed at low constant overpotentials, or at an initial high overpotential (to insure dendritic nucleation) which was subsequently reduced to a lower overpotential (to improve specific energy) at which dendritic growth could proceed without reverting to smooth deposition. The resulting current waveforms were recorded and the deposit morphology was determined.

The results with the scraped rotating cylinder electrode will not be shown because the set up was not considered satisfactory for practical application. The problems encountered were a) preferential growth of dendritic Zn at the fixed scraping blades, (b) IR losses and heating problems with the electrical contact to a moving electrode, and (c) unfavorably volume-to-area ratio of the reactor. Rather than attempting complicated solutions to maintain the rotating cylinder concept, a decision was made to develop a scraped planar electrode for a practical recharge cell in Phase III. In this design, the blades can be moved away during deposition to avoid preferential growth, the plate is fixed (only the scraper moves), simplifying mechanical drives and electric contacts, and the volume-to-area ratio is decreased. Lower recharge energies are expected with this design as well as easier scale up.

5.1 Recharge Studies.

A recharge study utilizing Mg and glassy carbon substrates was undertaken. The objective was to gather additional data to ex-

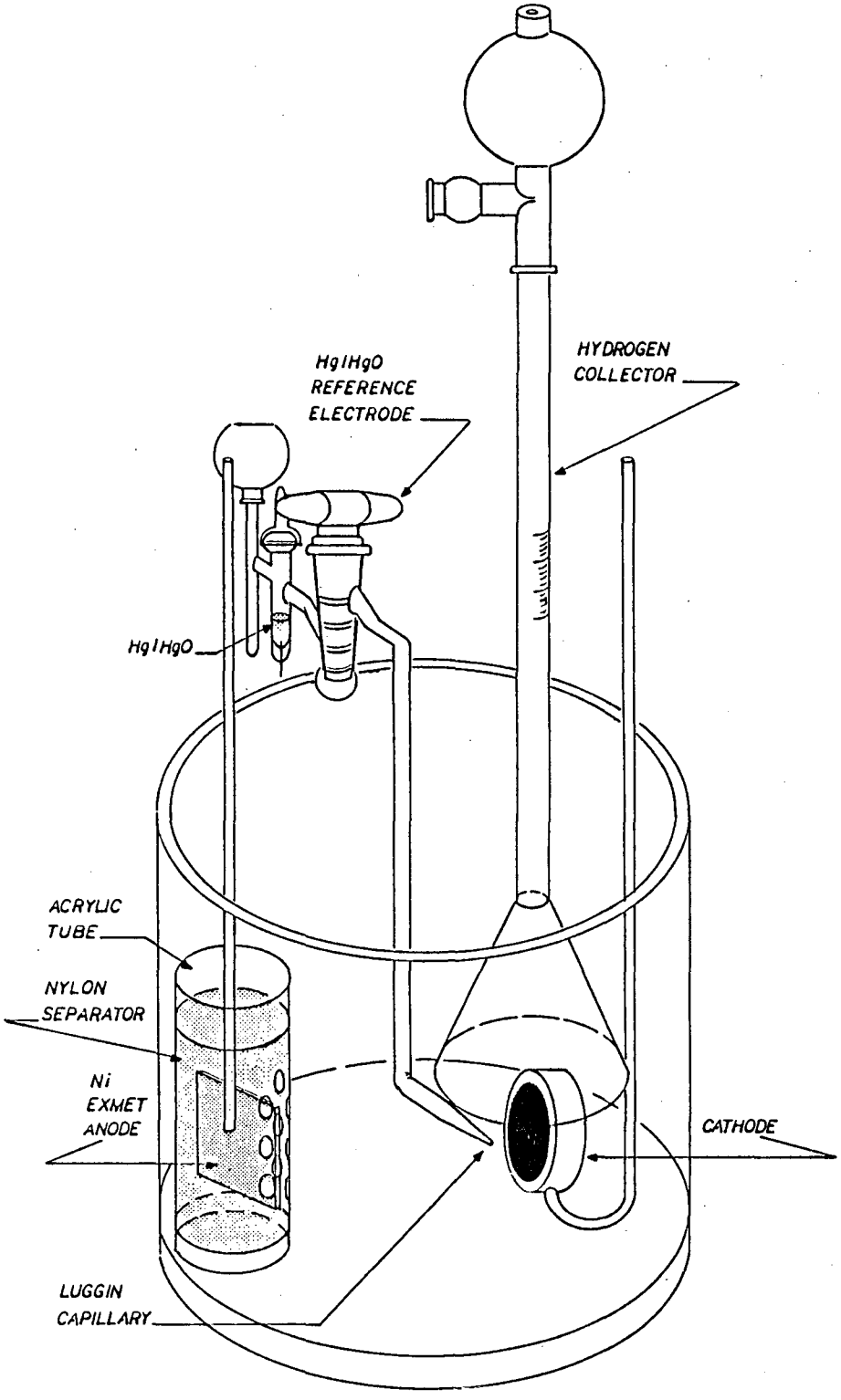

Fig. 14. Cell for recharge studies featuring a manually scraped planar cathode (Mg or GC) and dendrite net (not shown) to recover scraped Zn. Temperature control (not shown) was also featured.

plore the recharge of the slurry zinc-air battery by deposition of dendritic zinc in a planar electrode which is periodically scraped to produce a dendritic Zn powder. The parameters investigated included: (a) current density, (b) zincate concentration , (c) mass transfer rate, (d) temperature, (e) specific charge, and (f) current waveform (constant current or ramps with one or several current variation rates). The evaluation criteria were coulombic efficiency, half-cell specific energy, maximum half-cell power, and morphology of the scraped deposit (suitability for fluidization). Experiments were reported as half cell results because the cell and anode design were not optimized at this stage, experimental considerations are presented in section 5.2. The results of the recharge study are presented in Table 2 (page 25), and discussion of results is given in sections 5.3 to 5.11.

5.2 Manually Scraped Recharge Cell

The recharge of zincate oversaturated electrolyte was studied with the cell shown in Figure 14, in which the evolved hydrogen could be measured. The cathode substrates used were Mg and GC plates where dendritic Zn was deposited and scraped at periodic intervals with a polymeric blade. The anode was a nickel mesh. The cathode potential was measured with respect to a Hg/HgO reference electrode equipped with a Luggin capillary. Some anode potentials were also measured with respect to a similar reference electrode. A net was used to recover the scraped Zn for examination in a stereo microscope where the deposit microstructure was classified.

5.3 Coulombic Efficiency

The coulombic efficiencies were calculated from measurements of the evolved hydrogen and charge passed. Coulombic efficiency was calculated as a function of (a) concentration of zincate (depth of recharge), (b) concentration of discharge additive, (c) coulombs of charge passed (since the last scraping period) from 0 to 300 c/cm^2, (d) temperature, and (e) stagnant or stirred electrolyte. The structure of the deposit for each of the previous experiments was classified by stereo microscopic observation. The results shown in Figure 15 correspond to the time averaged values up to 300 c/cm^2 in quiescent electrolyte at room temperature. It can be seen that very high coulombic efficiencies (>99%) and relatively low overpotentials are possible for recharge at low current densities. The coulombic efficiencies are about the same for both Mg and GC substrates: above 99% at high zincate concen-

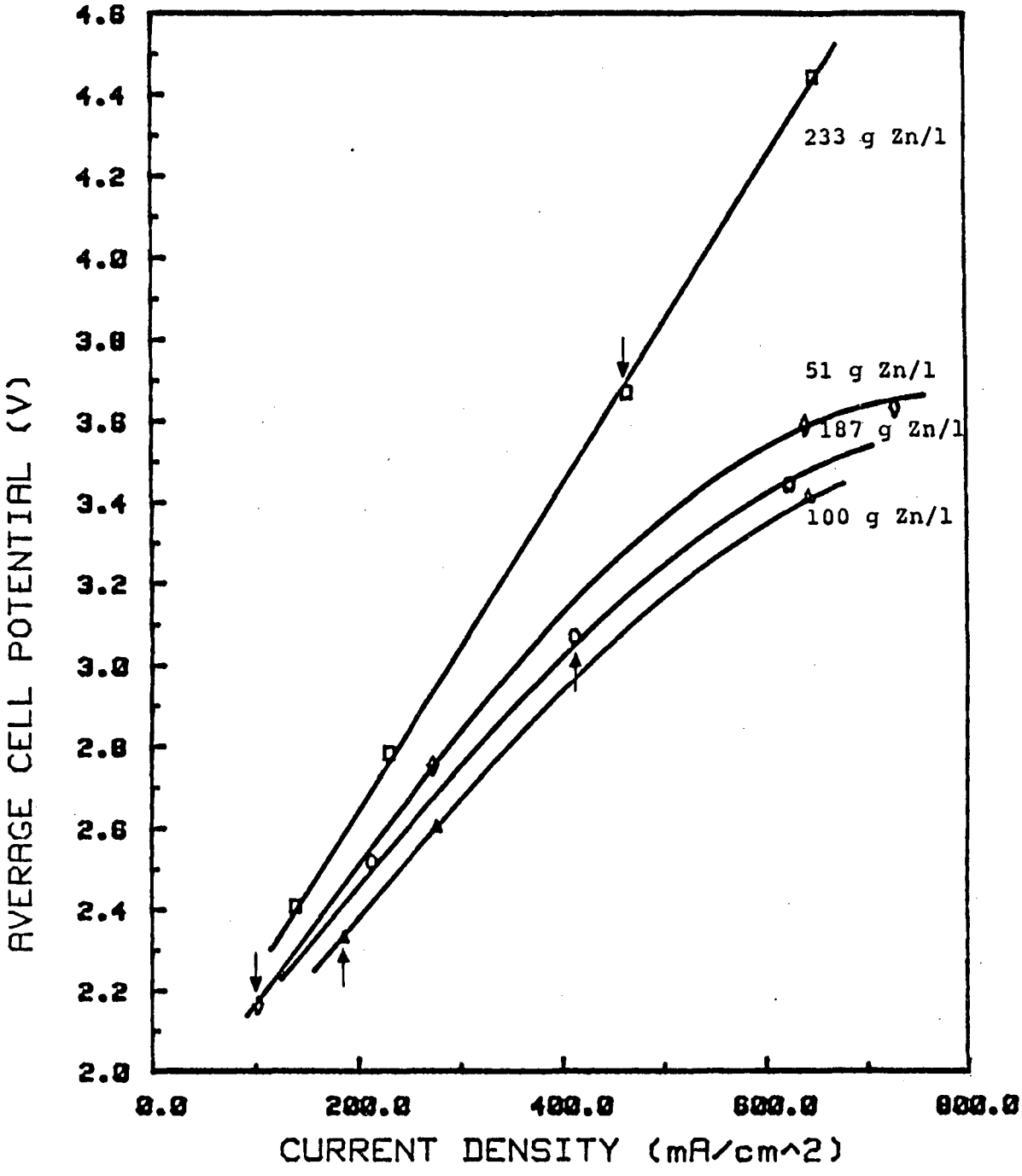

Fig. 16. Current density vs average cell potential. Recharge was performed at room temperature on a planar Mg disk with a total specific charge of 300 c/cm^2.

trations and down to about 88 % at 51 g Zn/l. These results apply in the current density range from 100 to 750 mA/cm^2. The effect of temperature on coulombic efficiency is discussed in section 5.7

5.4 Cell Voltage

The cell voltages obtained with a Mg cathode substrate and a Ni mesh anode are shown in Fig. 16. The arrows indicate the minimum current density at which a dendritic deposit is obtained. It can be seen that higher voltages are required to deposit dendritic Zn at both very high and very low concentrations of zincate ions in the solution. It is estimated that Zn dendrites are produced at average cell potentials below 2.3 V except during the first 10% of depth of charge (DoC). A current or potential waveform that varies with DoC can ensure minimum cell voltages and suitable dendritic Zn deposits. Cell voltage can be further decreased with better anode specification and cell design.

5.5 Current Density and Deposit Morphology

Dendritic Zn is deposited under diffusion controlled conditions which can be changed by adjusting the cathode potential. For galvanostatic deposition, the microstructure of the deposit is a function of the zincate ion concentration, the current density and the cathode substrate. Lower zincate concentrations, reduced electrolyte mass transfer rates and lower temperatures all favor the production of dendritic Zn that requires lower half-cell energy density, as shown in Table 2.

The lowest energy densities to charge with an acceptable dendritic morphology have been selected to operate the practical recharge cell planned to be built for Phase III. The best conditions imply operating at low current densities which vary with DoC.

5.6 Half Cell Energy Density

The average half-cell energy density (cathode overpotential times current density per gram of Zn produced) is plotted against current density in Figure 17 for constant current deposition at various DoC (expressed as grams of dissolved Zn per liter). The arrows indicate the lowest current density at which an acceptable dendritic Zn was deposited. It can be seen that the charge energy required has a minimum at DoC of about 100 g Zn/l. This occurs because higher voltages are required at low DoC in order to insure

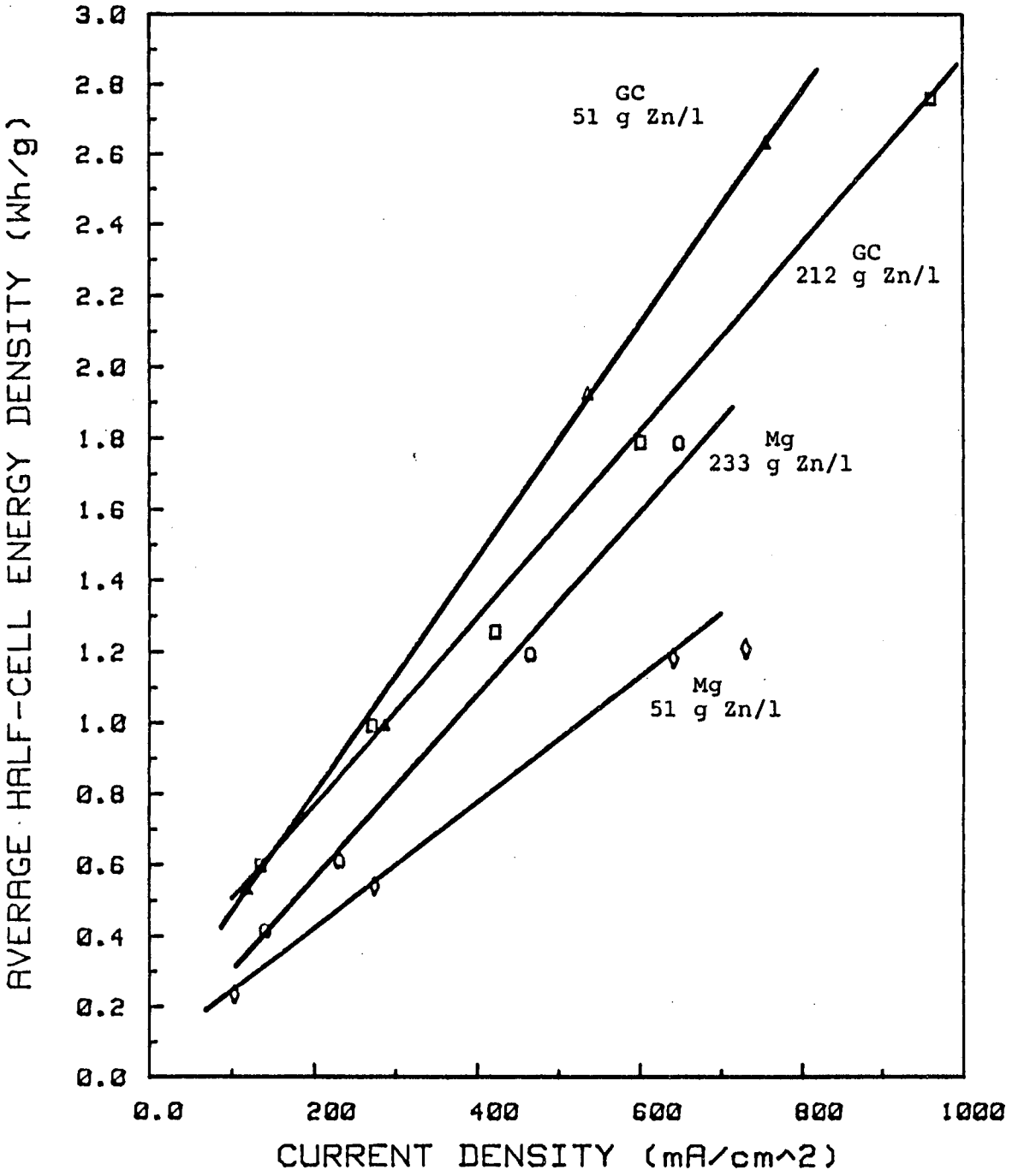

Fig. 17. Constant current density vs average half-cell energy density. Recharge was performed at room temperature on a planar Mg or glassy carbon disk. The total specific charge was 300 c/cm^2 except for GC, 212 g zn^{++}/l where the specific charge was 443 c/cm^2.

high currents for dendritic deposition (under diffusion control), and high DoC concentration polarization requires higher voltages, even at low current densities. Specific half-cell energies of less than 0.3 Wh/g Zn are feasible in the presence of LiOH additive.

5.7 Temperature Effects

The temperature of the electrolyte was found to decrease the time-averaged cathode potential at all depths of charge (Table 2). Figure 18 shows this effect with an electrolyte containing 51 g of dissolved Zn. However, at low current densities, a higher temperature promotes smooth Zn deposits. In Figure 18, the arrow indicates the only acceptable dendritic deposit at 101 mA/cm². Dendritic Zn was deposited at all higher current densities. Better performance was obtained at higher (70° C) temperatures, but a tendency towards smooth deposits can nullify this advantage.

The minimum current density, i_m, is that giving the lowest energy density with an acceptable deposit morphology. The i_m decreases with decreasing zincate ion concentration and increases with increasing temperature. For example, at low zincate concentrations (51 g Zn/l), i_m is 97 mA/cm² at 30 °C and about 266 mA/cm² at 70 °C. The half-cell energy density is nearly the same (0.22 Wh/g) at both temperatures.

Coulombic efficiency improved with temperature at all current densities, but the effect was more pronounced at the higher current densities (see Table 2). Smooth Zn is deposited at low current densities and higher temperatures, therefore the higher coulombic efficiencies can not be fully utilized because charging has to proceed at higher current densities in order to produce dendritic Zn at the higher temperatures. The optimum temperature and current density combination has to be determined by seeking the lowest specific recharge energy with acceptable deposit morphology. Extended measurements at low current densities, various temperatures and DoC need to be made for this purpose.

5.8 Hydrodynamic Conditions Effects

Preliminary evaluation of the recharge experiments shows better results were obtained in quiescent than in stirred electrolytes, insofar higher half-cell energy densities were required to produce dendritic deposits. The morphology under given constant current

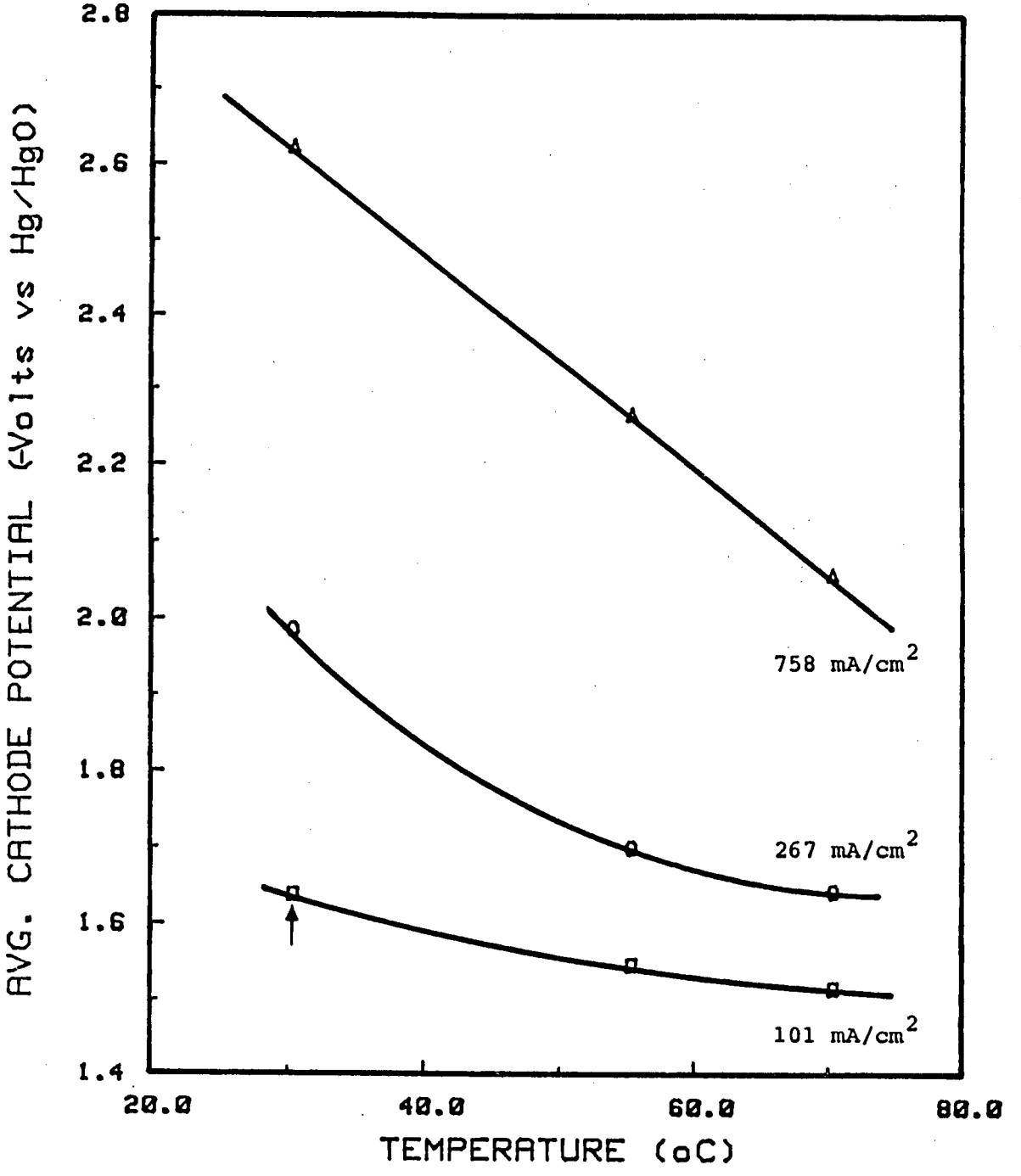

Figure 18. Average cathode potential vs. temperature curves for Zn deposition on Mg substrate at the indicated current densities. 300 c/cm^2 charge passed at a zincate concentration of 51 g Zn/l. The deposit morphologies on the 101 mA/cm^2 curve were not dendritic except that indicated by the arrow at 30° C.

deposition tended toward smooth deposits at higher stirring rates. Deposition under quiescent conditions is recommended for the practical recharge cell, with periodic flushing of scraped dendrites at time intervals extended as much as practical.

5.9 Current Waveform Effects

The coulombic efficiency and recharge energy can be conceivably improved by matching the current density to the real area of the deposit. Since the dendritic growth monotonically increases the electrode area, ramping the current was attempted at various ramping rates, rr. The results with the ramps are shown in Table 2 (the ramp rate, rr, in mA/cm^2, is printed below the current-density value). Most of the average current densities investigated were high because the possibility of rapid recharge with high coulombic efficiency was being explored. The results at various zincate ion concentrations and temperatures show that while high recharge rates are possible, no significant differences with the constant current recharge were observed in terms of coulombic efficiency and specific half-cell energy. It is recommended that the effect of current waveform shape be investigated at lower average current densities with the goal of decreasing the recharge specific energy.

In view of the effect of zincate ion concentration (DoC) on the morphology and specific half-cell energy, it is anticipated that although constant current might be employed for individual deposition cycles, the level of current density will be varied with DoC in order to minimize the overall recharge energy.

5.10 Cathode Substrate Effects

The chosen substrate for the recharge cell was Mg plate. Figure 17 shows that Zn deposition on Mg substrates require less energy than on GC. For example, an average half-cell energy density of 0.52 Wh/g was required for dendritic Zn deposition on Mg, while 0.98 Wh/g was required for GC while charging at ~ 280 mA/cm^2 from zincate ion solution containing 51 g Zn/l at room temperature. These differences are smaller at lower current densities and at higher zincate ion concentrations. The coulombic efficiencies of both substrates are similar to those shown in Figure 15.

Dendritic Zn deposition on Zn and Ni substrates was not successful because of adherence to the substrate.

Table 2. Performance and Characteristics of Zn Deposition in Quiescent Conditions

Experiments were performed galvanostatically with a 3.3 or 3.66 cm^2 magnesium electrode. Zincate was electrochemically saturated in 12M KOH solution with the aid of 25 g/l LiOH, unless otherwise noted. An electrolyte volume of 1 to 2 liters was used in all experiments to avoid depletion of Zn during recharge. The charge density was 300 c/cm^2 for all experiments.

Conc. of Zn^{++} (g/l)	††† Temp (°C)	Ave.* Current Density (mA/cm^2)	Cathode Over-potential (V)	Ave. Half-cell Power (W/cm^2)	Ave. Half-cell Energy (Wh/g)	Coulombic Efficiency (%)	** Structure
233	30	134 (c)	.487	.065	.400	99.99	(1), 2
233	30	225 (c)	.727	.164	.596	99.97	2 ,(3)
233	30	459 (c)	1.436	.659	1.178	99.96	3
233	30	642 (c)	2.160	1.387	1.772	99.95	(4), 5
233	30	729 (rr 3.6 $mA/sec\text{-}cm^2$)	1.803	1.314	1.479	99.99	4 ,(5)
233	30	1120 (rr 8.3 $mA/sec\text{-}cm^2$)	2.920	3.270	2.398	99.86	(5), 6
187†	30	208 (c)	.501	.104	.412	99.99	(2), 3
187†	30	407 (c)	.901	.366	.739	99.98	3
187†	30	619 (c)	1.193	.739	.979	99.94	(4), 5
187†	30	971 (c)	2.004	1.946	1.647	99.76	4 ,(5), 6
187†	30	701 (rr 3.3 $mA/sec\text{-}cm^2$)	1.584	1.110	1.299	99.98	(5), 6
187†	30	763 (rr 3.9 $mA/sec\text{-}cm^2$)	1.826	1.394	1.498	99.95	4 , 5
187†	30	900 (rr 5.5 $mA/sec\text{-}cm^2$)	1.911	1.720	1.568	99.98	5
149††	30	95 (c)	.193	.018	.158	99.89	(1), 2
149††	30	383 (c)	.924	.354	.759	99.80	2 ,(3)
149††	30	1546 (c)	1.971	3.048	1.659	97.45	(5), 6
149††	30	1141 (rr 8.7 $mA/sec\text{-}cm^2$)	1.492	1.702	1.238	98.80	(5), 6
100††	30	180 (c)	.326	.059	.268	99.70	3
100††	30	271 (c)	.492	.133	.406	99.48	4 ,(5)
100††	30	638 (c)	1.126	.718	.945	97.72	(5) 6
100††	30	696 (rr 3.3 $mA/sec\text{-}cm^2$)	1.150	.800	.969	97.29	5 ,(6)
100††	30	1128 (rr 8.8 $mA/sec\text{-}cm^2$)	1.605	1.810	1.382	95.21	6
51††	30	97 (c)	.259	.025	.214	99.32	5
51††	30	268 (c)	.606	.162	.519	95.50	5
51††	30	635 (c)	1.267	.805	1.160	89.56	6
51††	30	724 (c)	1.301	.941	1.186	89.98	6
51††	30	753 (c)	1.227	.924	1.130	89.06	6
51††	30	612 (rr 2.7 $mA/sec\text{-}cm^2$)	1.301	.796	1.255	85.01	6
51††	30	1025 (rr 7.4 $mA/sec\text{-}cm^2$)	2.179	2.233	2.378	75.16	6
51	55	101 (c)	.172	.017	.141	99.84	2
51	55	266 (c)	.323	.086	.266	99.44	4
51	55	492 (c)	.604	.297	.512	96.76	5
51	55	762 (c)	.890	.678	.769	94.96	5 ,(6)
51	55	726 (rr 3.6 $mA/sec\text{-}cm^2$)	1.052	.764	.937	92.08	ZnO
51	70	104 (c)	.141	.015	.115	99.90	2
51	70	266 (c)	.267	.071	.220	99.57	4
51	70	496 (c)	.432	.214	.359	98.70	4 ,(5)
51	70	758 (c)	.683	.517	.576	97.12	5 ,(6)
51	70	744 (rr 3.6 $mA/sec\text{-}cm^2$)	.748	.556	.623	98.42	5 ,(6)

* (c) Constant current (rr) Ramp rate

** Structure of Zn deposits:
1) Smooth
2) Mossy
3) Bulbous dendrite
4) Disc shape dendrite
5) Fern leaf dendrite
6) Small fern leaf dendrites clustered together

(The number in parentheses represents the majority.)

† 25 g/l silicate + 15 g/l sorbitol was used as the additive

†† 5 g/l LiOH was used as the additive

††† 30°C indicates the average electrolyte temperature. The actual range for the experiments was 22 to 34°C.

5.11 Effect of Discharge Additives

There was a concern that the improved stability of zincate ions or ZnO in solution containing LiOH and other capacity extension additives would make the recharge process more difficult. This work concludes that production of dendritic Zn from oversaturated zincate solutions stabilized with LiOH is feasible and can proceed with low energy requirements. The benefits are not necessarily extended to other Zn-air systems with static or flowing electrolyte because of the unique characteristics of the slurry system that involve a fluctuating discharge potential coupled with brisk hydrodynamic conditions on discharge and dendritic rather than smooth Zn deposition on recharge under quiescent conditions.

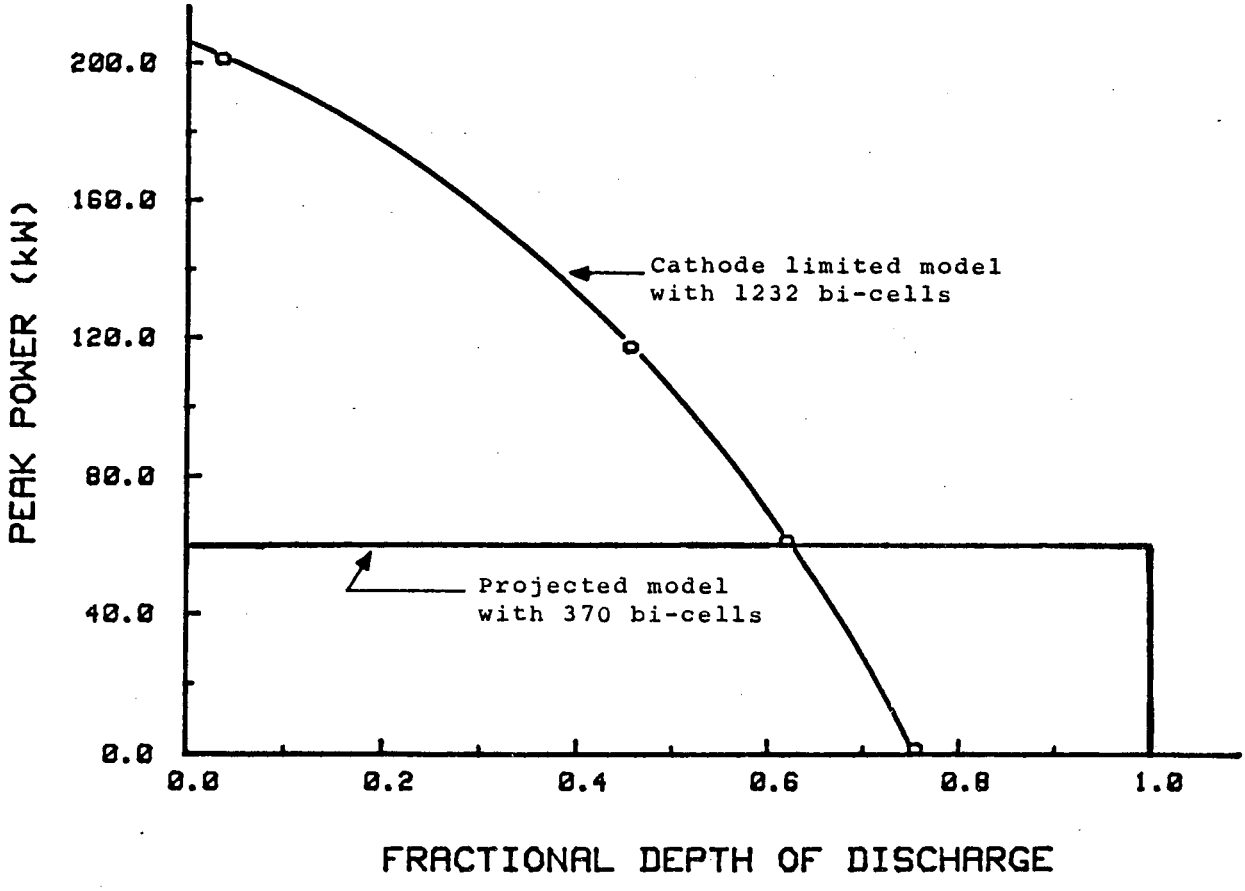

Figure 19. Peak power vs. fractional depth of discharge of two secondary slurry-Zn/air battery packs for the IDSEP van. The model limited by air cathode passivation needs 1232 bi-cells, the projected model with no air cathode passivation needs only 370 cells to sustain 50 kW peak power.

6. MODELING OF SLURRY-Zn/AIR BATTERY SYSTEMS

6.1 11-KW Hydraulically Recharged Slurry-Zn/Air Battery System

Single-cell charge and discharge experiments using both Zn powder slurry and Zn-coated polymeric bead (Sorapec Bead) slurry, and silicate + sorbitol additive were used as the basis for a 11 kW, 300 kg slurry-Zn/air battery model, featuring a stack of bi-cell II's. The best Ragoné curve (for Zn powder slurry and oxygen depolarization) results in 105 W/kg and 47 kWh/kg for short range missions and 465 kWh and 24 W/kg for long range missions. An extended description and comparison of various 11 kW systems based on experimental results with bi-cells I and II, and tubular cells from the CGE slurry-Zn/air battery under various additives and polarization conditions has been published (5).

6.2 60-KW Hydraulically Recharged Slurry-Zn/Air Battery System

Single-cell charge and discharge experiments (with LiOH additive) were used to estimate an energy density of 140 Wh/kg, and 64 kWh for a 700 kg battery system with a maximum power of 60 kW and a cruise power of 5.5 kW. The hydraulically recharged battery system was calculated as requested by DOE in a report submitted to Sheladia Associates Inc (6). With some reasonable extrapolations, a specific energy of 180 Wh/kg at a power density of 66 W/kg was projected for a battery pack for the IDSEP van slurry-Zn/air battery, occupying less than 600 l.

6.3 50-KW Slurry-Zn/Air Battery System with On-Board Recharge

Models of a secondary slurry Zn-Air battery system with on-board and hydraulic recharge based on single-cell experimental data using LiOH additive are described in this section. The criteria for modeling the battery system was that 5.5 kW cruising power and 50-kW peak power should be always available within the DoD chosen, and that the battery weight should not exceed 755 kg. This battery system is similar to the battery pack required to power the 2000 kg IDSEP van, and only differs by the on-board recharge capability added to the hydraulic recharge capability (central recharge).

Two battery system models with on-board recharge were calculated. In one model (projected model) the initial (zero DoD) peak power was assumed constant through 100% DoD, the other assumption

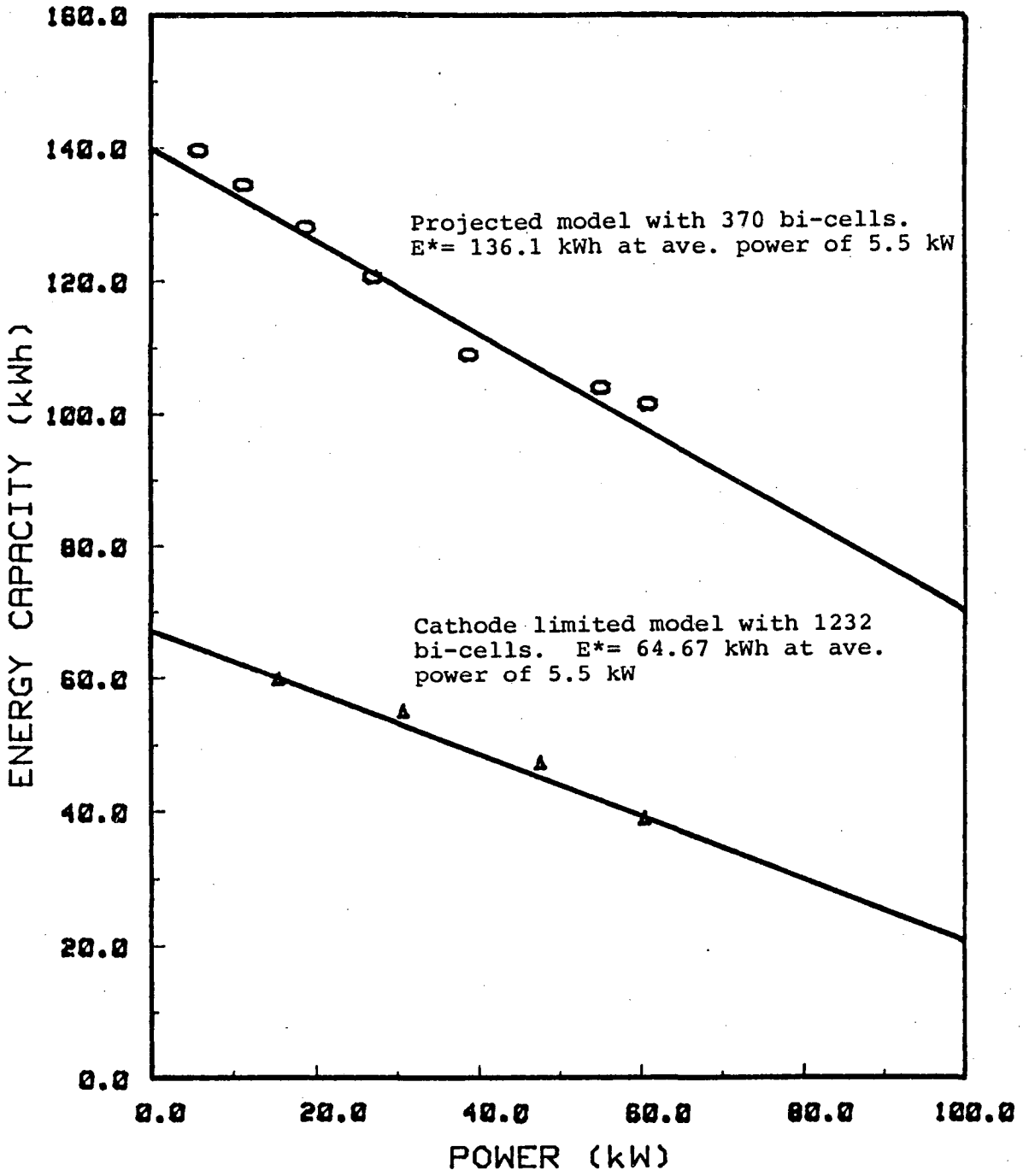

Figure 20. Ragoné plots of secondary slurry-Zn/air battery packs described in Figure 19. The projected pack with no air cathode passivation could give 136.1 kWh at 5.5 kW cruising power.

was that the highest IDC obtained experimentally (302 Ah/l) was 100% DoD. In the second (air-cathode-limited model) the capacity used in the model was only 60% of the IDC for two reasons: 1) air cathode passivation determined the end of discharge at 228 Ah/l (75% of the IDC capacity in bi-cell II), and 2) a compromise capacity of 65% of IDC capacity had to be chosen to achieve a reasonable specific peak power. The peak power decreased with increasing DoD according to the experimental values taken with bi-cell II (Figure 13). Only the initial peak power was used for the projected model but all of the curves in Figure 13 were used for the air cathode limited model.

The highest peak power, 810 mW/cm², was measured at the start of discharge (16 Ah/l)in Figure 13. This value was used in the calculations of a projected model with 370 bi-cells. In this projected model a maximum peak power of at least 810 mW/cm² is expected to be available at all times, until passivation of the Zn particles in the slurry occurs, provided that the air cathode is protected from premature passivation. The peak power vs. fractional depth of discharge curve for this projected model is shown in Figure 19 as a constant 50-kW until passivation of the Zn slurry (fractional DoD =1).

The maximum specific peak power (Figure 13) continually decreases down to 243 mW/cm² at 65% DoD, due primarily to passivation of the air cathode. This peak power was used to calculate the size of the discharge reactor. The air cathode limited model needed 1232 bi-cells in order to meet the requirement of 50 kW peak power. 65% DoD was the value used as operating capacity since at higher DoD the peak-power requirement was not fulfilled. The peak power vs. fractional DoD curve for the air cathode limited model is shown in Figure 19. It can be noted that up to four times excess peak power is available at the beginning of discharge.

The weight and volume breakdown of the projected battery system is given in Table 3. The weight of the system without the slurry is estimated to be 197.5 kg. A discharge stack comprising 370 bi-cells with 200 cm² of air cathode each is estimated to weigh 92.5 kg. Miscellaneous components, including air system (intake funnel, filter and housing, humidifier/scrubber, shroud, water tank, valves, air pump), electrolyte system and controls (holding tank, reactor pumps, intermodular plumbing, sensors and valves) mountings and oxygen gained (from air to ultimately form zincate or ZnO) are estimated to weigh 50 kg. The recharge stack composed of 24 Mg plate cathodes and 25 anodes

with 5000 cm^2 area each is estimated to weight 55 kg. In view of the relatively small weight of the battery hardware, 557.5 kg (345 l) of electrolyte slurry can be carried on board.

The estimated weight of the air-cathode-limited battery system without slurry electrolyte is 408 kg, leaving only 342 kg (212 l) for the slurry electrolyte. The total volume of both systems is estimated to be less than 550 l.

TABLE 3. PRI SECONDARY SLURRY ZINC-AIR ON-BOARD RECHARGE MODEL

WEIGHT:	
WEIGHT OF BATTERY COMPONENTS:	
DISCHARGE CELL	
370 BI-CELL (200 CM^2/BI-CELL)	92.5 KG
RECHARGE CELL	
24 BI-CATHODE (5000 CM^2/BI-CATHODE)	52.0 KG
25 BI-ANODE (5000 CM^2/BI-ANODE)	3.0 KG
MISC:	50.0 KG
AIR OPERATING SYSTEM (INTAKE FUNNEL, FILTER AND HOUSING, HUMIDIFIER/SCRUBBER, SHROUD, WATER TANK, VALVES, AIR PUMP), ELECTROLYTE OPERATING SYSTEM (HOLDING TANK, REACTOR, PUMPS, INTERMODULAR PLUMBING, VALVES), CONTROL, SENSORS, MOUNTINGS, OXYGEN GAINED.	
WEIGHT OF ELECTROLYTE:	
345.7 LITERS OF SLURRY ELECTROLYTE	557.5 KG
	755.0 KG
VOLUME:	
DISCHARGE REACTOR	19.0 L
HOLDING TANK #1 (INCLUDING RECHARGE CELL)	382.0 L
HOLDING TANK #2	65.0 L
MISC:	50.0 L
(AIR OPERATING SYSTEM, ELECTROLYTE OPERATING SYSTEM, CONTROL, SENSORS, MOUNTINGS)	
	516.0 L

The models presented propose separate charge and discharge cells (Figure 1), where the function of each can be optimized for energy and coulombic efficiencies, rather than utilizing a bifunctional electrode approach for the secondary battery system.

The size of the discharge and recharge stacks is small, compared with the volume of slurry needed for typical EV applications. The projected discharge stack is composed of planar bi-cells with air feed to the inner compartment of each bi-cell, as has been described previously. The slurry circulates with high turbulence through the gaps between the bi-cells connected in parallel inside a submodule. The series-connected submodules are envisioned to have separate electrolyte flows to reduce the shunt current losses. The projected recharge cell stack is located in the main electrolyte tank (Tank No. 1 in Figure 1) under near quiescent hydrodynamic conditions. Recharge cells are formed by Mg plates where dendritic Zn is deposited and mechanically removed at periodic intervals with a polymeric blade that scrapes the surface of the Mg cathode. The anode for the recharge cell is a nickel mesh for oxygen evolution. Hydrogen depolarization of the anodic recharge cell is envisioned only for central recharge stations because of practical and safety-related issues that on-board use would raise. Hydrogen is a cheaper energy source than electricity and reduces the electrical energy needed for recharge to less than 50% of that available from the fully recharged slurry.

Table 4. Projected Recharge Performance Of The Secondary Slurry Zn/Air Battery

	Ave. Current Density (mA/cm^2)	Ave. Cell Potential (V)	Coulombic Efficiency (%)	Voltage Efficiency (%)*	Energy Efficiency (%)*,†
On-board Recharge					
Slow Charge	163	2.414	99.66	54	47
Fast Charge	638	3.754	95.38	35	29
Ramp Charge ($3.3\ mA/sec \cdot cm^2$)	700	3.862	97.98	34	29
Central Recharge (H_2 anode)	75	0.760	NA	NA	52††

* Voltage Efficiency, and Round Trip Energy Efficiency were calculated based on discharge potential of 1.3 V at 100 mA/cm^2 and discharge coulombic efficiency of 96.89%

† Round Trip Energy Efficiency was including pumping loss, shunt current loss, and self discharge

†† Energy Efficiency was calculated based on the theoretical combustion energy of hydrogen and electrical energy required for slow charge

In Figure 20 two Ragoné-type curves describe the performance of the projected (370 bi-cells) and cathode-limited (1232 bi-cells) secondary battery systems. The 1232 bi-cell system can only carry 212 l of slurry electrolyte (342 kg) to complete the 755 kg total weight. Therefore, E*, the available energy at cruising power is only 64.67 kWh, compared with 136.1 kWh available with the projected 370 bi-cell model.

The energy density at 5.5 kW projected for the secondary slurry-Zn/air battery system is estimated to be 180 Wh/kg (7). A summary of the estimated recharge performance is given in Table 4, and a cost estimation of the energy required for recharge is given in Table 5. For slow recharge, the round-trip efficiencies are >99% coulombic efficiency, 54% voltage efficiency and 47% energy efficiency. Thus the estimated cost of energy is $0.14 /kg of Zn recharged with off-peak electrical energy at $0.07/kWh. If the recharge anode is depolarized with H_2, which costs $1.67/100 SCF, the cell voltage can be reduced to 0.7 V at 75 mA/cm^2 and therefore the consumption of electrical energy is reduced and the total cost of recharge energy is then only $0.06/kg of Zn. This means a cost of only $0.056/kWh when using central-station recharge aided with H_2. A gross estimate of the battery cost is $3000. We have presently no data to estimate the life of the battery but, in principle, it should last as long as the vehicle.

Table 5. Projected Cost Analysis of the Secondary Slurry Zn-Air Battery

	Energy Cost	
	Recharge Cost ($/kg) ††	Cost per kwh ($/kwh) †
Slow Charge	0.14	0.13
Fast Charge	0.23	0.21
Ramp Charge	0.23	0.21
H_2 Anode Charge	0.06	0.056

† Energy Consumption Cost was calculated based on an energy density of 1.07 kwh/kg.

†† Reproduction Energy Cost was calculated based on off peak-hour electricity cost (0.07 $/kwh), and Hydrogen production cost through electrolysis of water ($1.67/100 SCF).

ACKNOWLEDGEMENT

This work was supported by the Assistant Secretary for Conservation and Renewable Energy, Office of Energy Storage and Distribution of the U.S. Department of Energy under Contract No. DE-C03-76SF00098, Subcontract No. 4543210, with the Lawrence Berkeley Laboratory.

REFERENCES

1. H.B. Sierra Alcázar, P.D. Nguyen, and A.A. Pinoli, Final Report of Technology Base Research on Zn/Air Battery Systems, Lawrence Berkeley Laboratory, Rept. LBL-23960 (1987)
2. H.B. Sierra Alcázar and P.D. Nguyen, "Additives to Increase the Discharge Capacity of the Moving Bed Zn-Air Battery". Proceedings of the 22nd Intersociety Energy Conversion Engineering Conference, Paper 879397, Philadelphia PA, August 10-14, 1987.
3. H.B. Sierra Alcázar and P.D. Nguyen, "Technology Base Research on the Slurry Zn-Air Battery ". Proceedings of the 172nd Electrochemical Soc. Meeting., Honolulu, HI, October 19-23, 1987.
4. H.B. Sierra Alcázar, P.D. Nguyen, and A.A. Pinoli, "Slurry Zn-Air Battery Research and Development". Proceedings of the 8th DOE Battery and Electrochemical Contractors Conference, Vienna, VA, November 19, 1987.
5. H.B. Sierra Alcázar and P.D. Nguyen, Progress In Batteries and Solar Cells, **7**, 21 (1988).
6. H.B. Sierra Alcázar and P.D. Nguyen."Projected Performance of a Slurry Zn-Air Battery for the IDSEP Van" Report submitted to Sheladia Associates Inc. for the Department of Energy, (1988).
7. H.B. Sierra Alcázar, P.D. Nguyen, A.A. Pinoli, "The Secondary Slurry Zn-Air Battery for EV Propulsion" Proceedings of the 33rd International Power Sources Symposium, Cherry Hill, NJ, June 13-16, 1988.
8. H.B. Sierra Alcázar, P.D. Nguyen, A.A. Pinoli," Performance of Slurry-Zn/Air Recharge and Discharge Cells with KOH-LiOH Electrolyte" Extended Abstract Proceedings of the 174th Meeting of the Electrochemical Society, Chicago, IL, October 9-14, 1988.

LAWRENCE BERKELEY LABORATORY
TECHNICAL INFORMATION DEPARTMENT
UNIVERSITY OF CALIFORNIA
BERKELEY, CALIFORNIA 94720

AAF411
LBL Libraries